

Experimental *Mycobacterium tuberculosis* Infection of Cynomolgus Macaques Closely Resembles the Various Manifestations of Human *M. tuberculosis* Infection

Saverio V. Capuano III,^{1,2} Denise A. Croix,^{1†} Santosh Pawar,¹ Angelica Zinovik,¹
Amy Myers,¹ Philana L. Lin,³ Stephanie Bissel,⁴ Carl Fuhrman,⁵
Edwin Klein,⁶ and JoAnne L. Flynn^{1*}

Departments of Molecular Genetics and Biochemistry,¹ Obstetrics, Gynecology, and Reproductive Sciences,² Pathology,⁴
and Radiology⁵ and Division of Laboratory Animal Resources,⁶ University of Pittsburgh School of Medicine,
and Department of Pediatrics, Children's Hospital,³ Pittsburgh, Pennsylvania 15261

Received 28 February 2003/Returned for modification 6 May 2003/Accepted 21 July 2003

Nonhuman primates were used to develop an animal model that closely mimics human *Mycobacterium tuberculosis* infection. Cynomolgus macaques were infected with low doses of virulent *M. tuberculosis* via bronchoscopic instillation into the lung. All monkeys were successfully infected, based on tuberculin skin test conversion and peripheral immune responses to *M. tuberculosis* antigens. Progression of infection in the 17 monkeys studied was variable. Active-chronic infection, observed in 50 to 60% of monkeys, was characterized by clear signs of infection or disease on serial thoracic radiographs and in other tests and was typified by eventual progression to advanced disease. Approximately 40% of monkeys did not progress to disease in the 15 to 20 months of study, although they were clearly infected initially. These monkeys had clinical characteristics of latent tuberculosis in humans. Low-dose infection of cynomolgus macaques appears to represent the full spectrum of human *M. tuberculosis* infection and will be an excellent model for the study of pathogenesis and immunology of this infection. In addition, this model will provide an opportunity to study the latent *M. tuberculosis* infection observed in ~90% of all infected humans.

Tuberculosis is responsible for more than 2 million deaths worldwide each year. This disease and the causative agent *Mycobacterium tuberculosis* have been intensively studied, yet the basis for protection, as well as many of the microbial and immunologic factors that contribute to disease, is not well understood. The lack of an efficacious vaccine hampers control of this disease, and although effective drug treatment exists, the regimens are lengthy and involve multiple drugs, some with considerable toxicity. Further research to identify mechanisms of protection, as well as strategies for vaccine and drug development, is necessary to combat this worldwide problem.

M. tuberculosis infection in humans does not usually lead to active disease. The majority of infections are clinically latent, with only ~10% of those infected progressing to active tuberculosis. Latent tuberculosis in humans is defined as no signs of clinical disease in a purified protein derivative-positive (PPD⁺) person. Latently infected persons likely harbor the organism for life and carry a risk for reactivation tuberculosis. The immune responses that lead to control of acute infection and possibly establishment of latency have begun to be determined using animal models (10). However, since true latent infection is not observed in the standard animal models of tuberculosis, it is challenging to study the process by which this occurs, and the many factors involved in reactivation are difficult to identify.

Animal models have been used extensively to dissect the host response to infection, as well as the pathogenesis of the microbe. Each animal model has advantages and disadvantages (9). Most commonly used is the murine model. Mice can be infected via aerosol with a low dose of organisms, which multiply in the lungs and spread to other organs, most notably the spleen and liver. This infection is controlled, but not eliminated, by cell-mediated immunity, primarily T-cell responses. The ensuing chronic infection is reasonably well tolerated for more than a year in some mouse strains (10). The murine model is extremely attractive for many reasons, including low cost compared to larger animal models, relative ease of biocontainment, availability of reagents, reproducibility of the infection, and existence of susceptible, inbred and genetically altered mouse strains. The immune response to *M. tuberculosis* in the mouse has been shown to have direct correlates in the human system, including the importance of CD4 T cells (3, 17, 21), interleukin-12 (5, 8), and tumor necrosis factor alpha (2, 11, 13, 16). Nevertheless, there are aspects of the murine infection that do not closely mimic human disease, including the relatively high bacterial burden maintained in the lungs and spleen during the chronic stage (18) and the pulmonary pathology. Mice do not exhibit classical tuberculous granulomas in the lungs; there are collections of lymphocytes and macrophages that form and act to contain the infection, but these lack the well-formed structure of human granulomas (19). In addition, mice do not develop pulmonary cavities, an important feature of human tuberculosis that directly contributes to the spread of infection.

Both the guinea pig and rabbit models have been used in

* Corresponding author. Mailing address: Department of Molecular Genetics and Biochemistry, University of Pittsburgh School of Medicine, W1157 Biomedical Science Tower, Pittsburgh, PA 15261. Phone: (412) 624-7743. Fax: (412) 648-3394. E-mail: joanne@pitt.edu.

† Present address: Miltenyi Biotec, Inc., Auburn, CA 95602.

TABLE 1. Monkeys infected with *M. tuberculosis* and outcome to date

Monkey no.	Date of birth (mo/day/yr)	Wt at infection (kg)	Date of infection (mo/day/yr)	Status during infection	Date of euthanasia (mo/day/yr)	Status at euthanasia (or present status)
71-00	1/9/96	4.3	4/19/01	Active-chronic	6/22/01	Moderate disease
72-00	1/1/96	5.1	4/19/01	Active-chronic	2/01/02	Advanced disease
144-00	10/7/95	6.5	4/19/01	Latent		Alive, no signs of disease
145-00	9/18/94	8.1	4/19/01	Latent		Alive, no signs of disease
146-00	8/14/95	5.3	4/19/01	Latent	8/15/01	No disease, a few tiny granulomas
150-00	10/12/93	3.8	4/19/01	Active-chronic	8/08/01	Moderate disease
151-00	6/17/94	3.5	4/19/01	Active-chronic	8/13/01	Moderate disease
152-00	7/12/93	3.1	3/30/01	Active-chronic	6/19/02	Minimal disease
153-00	4/30/93	3.8	3/30/01	Rapid progressor	6/11/01	Advanced disease
109-01	1/1/93	9.5	9/4/01	Latent		Alive, no signs of disease
110-01	2/1/93	9.7	9/4/01	Latent		Alive, no signs of disease
111-01	3/1/93	9.1	9/4/01	Latent		Alive, no signs of disease
112-01	2/1/93	9.7	9/4/01	No signs, then rapid onset	5/30/02	Advanced disease
113-01	2/1/93	7.5	9/4/01	Active-chronic	4/25/02	Advanced disease
114-01	1/1/93	8.3	9/4/01	Active-chronic		Alive, mild active disease
115-01	1/1/93	7.5	9/4/01	Latent		Alive, no signs of disease
116-01	3/1/93	7.3	9/4/01	Active-chronic		Alive, very mild disease

tuberculosis research. These animal models mimic some features of human disease including lung granulomas that more closely resemble the human lung pathology, including cavity formation in rabbits (7, 13, 15). However, there is little available information on whether latent tuberculosis can be modeled in these animals. Furthermore, the study of the immune response in guinea pigs and rabbits has been hampered by the lack of appropriate reagents, as well as the difficulty in obtaining inbred strains, although some of these reagents are being developed.

The nonhuman primate model of tuberculosis has a long history. Monkeys were used for tuberculosis research for many years, for vaccine and drug efficacy studies (1, 12, 22–24). However, for various reasons, including cost and biocontainment, the monkey model has been rarely used in the past 30 years. Much of the information regarding *M. tuberculosis* infection in primates comes from outbreaks within primate colonies (6, 25, 32, 33). In 1996, Walsh et al. published data demonstrating that inoculation of macaques with a low dose of *M. tuberculosis* did not necessarily result in fulminant disease and raised the possibility that macaques may be an excellent model of human tuberculosis (30). In addition, major advances in the availability of immunologic and other reagents for use in macaques, pioneered primarily by those studying simian immunodeficiency virus infection in macaques as a model for human immunodeficiency virus infection and AIDS, have made the study of host responses in monkeys feasible. Recently, a limited number of studies using macaques for tuberculosis research have appeared (14, 26), suggesting a new interest in the use of this model. While the difficulties and expense of performing research under biosafety level 3 containment with *M. tuberculosis*-infected nonhuman primates limit the widespread use of this model, it appears to have some distinct advantages over other model systems, including potential applicability to human disease, as well as the possibilities for *M. tuberculosis*-simian immunodeficiency virus coinfection models.

The immediate goal of this research was the development of a model of human tuberculosis in macaques. We demonstrate here that cynomolgus macaques can be reproducibly infected

with very low doses of *M. tuberculosis* delivered to the lungs via flexible bronchoscope. We monitored the monkeys for 15 to 20 months in some cases, and the spectrum of disease observed in our monkeys resembles that seen in humans. Monkeys developed either rapid-onset fulminant disease, active-chronic disease, or no disease. Those animals with no clinical signs of disease may have latent infections and provide a model for the study of latency and reactivation. Thus, this model provides a unique opportunity for study of various aspects of human tuberculosis.

MATERIALS AND METHODS

Experimental animals. Seventeen adult, simian retrovirus type D-negative cynomolgus macaques ranging in age from 5 to 8 years (Table 1) and weighing 3.1 to 9.7 kg were used for this study. The animals were supplied by Three Springs Scientific (Perkasie, Pa.) and are of Philippine or Chinese origin; animals were resident in the United States prior to our purchase of them. Prior to the commencement of the study, the 6 female and 11 male macaques underwent a rigorous battery of diagnostic procedures (e.g., physical exam, complete blood count with differential, erythrocyte sedimentation rate [ESR], serum chemistry profile, direct fecal exam, rectal culture, thoracic radiography, lymphocyte proliferation assays [LPAs], and tuberculin skin testing) to ensure that they were free of any underlying disease processes, especially mycobacterium infection. All animals were individually housed in 4.3-ft² stainless steel cages equipped with Lexan fronts to reduce the potential for aerosol contact between animals. All cages were maintained within a negatively pressurized BioBubble (Colorado Clean Room Company) located within a biosafety level 3 suite. All animal manipulations were performed in a dedicated procedure area of the BioBubble. All animal experimentation guidelines were followed in these studies, and all experimental manipulations and protocols were approved by the University of Pittsburgh School of Medicine Institutional Animal Care and Use Committee.

Bacteria. *M. tuberculosis* strain Erdman, a virulent strain, was used for all infections. This strain was originally obtained from the Trudeau Institute, passaged through mice, and stored in aliquots at –80°C. A frozen aliquot was diluted in sterile saline, cup-horn sonicated for 15 s, and diluted to the appropriate concentration for infection. An aliquot of the dilution used for infection was plated on 7H10 agar plates to determine bacterial numbers in the sample.

Experimental infection and BAL procedures. To prepare for infection or bronchoalveolar lavage (BAL), a 2.5-mm-outer-diameter flexible fiber optic bronchoscope (Richard Wolf Veterinary Products, Chicago, Ill.) was disinfected in Cidex (Johnson & Johnson, Irvine, Calif.) for 15 min prior to use and between animals. After disinfection, the outer surface and the biopsy channel of the bronchoscope were rinsed thoroughly with sterile 0.9% saline. Prior to infection and diagnostic BAL, all animals were anesthetized with an intramuscular dose of 10 mg of ketamine (Phoenix Pharmaceuticals, St. Joseph, Mo.)/kg of body weight or 5 to 8 mg of tiletamine-zolazepam (Telazol; Fort Dodge, Fort Dodge, Iowa)/

kg. Animals also received 0.04 mg of atropine (Phoenix Pharmaceuticals)/kg intramuscularly to reduce salivary secretions and to inhibit the occurrence of bradycardia. Once sufficiently anesthetized, animals were placed in dorsal recumbency on an exam table and preoxygenated with 100% oxygen via face mask. To facilitate the insertion of the bronchoscope into a segmental bronchus of the right middle or right caudal lung lobe, cetacaine (Bergen Brunswig, Carrollton, Tex.) was applied topically to the epiglottis and the vocal folds via a spray bottle and 1 to 5 ml of 1% lidocaine (Bergen Brunswig) was applied to the mucosa of the trachea at the level of the carina via the biopsy channel of the bronchoscope. For infection, the bronchoscope was wedged into the desired segmental bronchus, and ~25 CFU of *M. tuberculosis* Erdman strain in 2 ml of sterile saline was instilled into the right caudal or right middle lung lobe via the biopsy channel of the bronchoscope followed by 3 ml of sterile saline. For BAL, the bronchoscope was wedged into the desired segmental bronchus, and four individual 10-ml aliquots of sterile 0.9% saline were instilled into and aspirated from the lung via the biopsy channel of the bronchoscope. Postinfection and post-BAL animals were oxygenated via face mask and were monitored closely until they recovered completely from anesthesia.

Tuberculin skin testing procedures. The palpebral area has been traditionally used for tuberculin skin testing of monkeys because it is easy to visualize the results of the test without anesthetizing or restraining the animals. The abdomen is sometimes used because it provides a large area where several types of tuberculin (e.g., mammalian tuberculin, PPD, *Mycobacterium avium* PPD, and saline) can be placed for comparison of reactions. Intradermal palpebral skin testing was performed using 0.1 ml of mammalian tuberculin (Synbiotics, San Diego, Calif.). Intradermal abdominal skin testing was performed with 0.1 ml of mammalian tuberculin, 0.1 ml of 0.9% sterile saline, and 0.1 ml of PPD spaced equidistantly in a triangular pattern on the abdomen. Monkeys were anesthetized intramuscularly with ketamine (10 mg/kg) for administration of the skin test (during normal physical exam) and to measure the abdominal test at 48 and 72 h. Palpebral reactions were graded at 24, 48, and 72 h with the standard 1 to 5 scoring system (20). In this system, 0 equals no reaction observed, 1+ equals bruise, 2+ equals various degrees of erythema without swelling, 3+ equals various degrees of erythema with minimum swelling or slight swelling without erythema, 4+ equals obvious swelling of palpebrum with drooping of eyelid and various degrees of erythema, and 5+ equals swelling and/or necrosis with eyelid closed. Abdominal indurations at each test site were measured (in millimeters) with a Vernier caliper at 48 and 72 h.

Radiographic procedures. Ventral-dorsal and right lateral thoracic radiographs were taken using a portable radiographic unit (Tri-State Medical Supplies, Pittsburgh, Pa.), with Green Sensitive Rare Earth film. Radiographs were taken immediately prior to infection; 2, 4, 6, and 8 weeks postinfection; and monthly to bimonthly thereafter. Radiographs were also taken when clinically necessary and immediately prior to euthanasia and were read by a board-certified thoracic radiologist with extensive experience in pulmonary tuberculosis (C.F.).

Blood collection procedures. All blood samples were collected via femoral venipuncture with Vacutainer needles (22 gauge), needle holders, and blood collection tubes while the animals were under ketamine or tiletamine-zolazepam anesthesia.

Gastric aspirate collection and culture procedures. Fluid was aspirated from the stomach by using a red rubber feeding tube and a 5-ml syringe. In some monkeys, 5 ml of saline was first delivered to the stomach via the feeding tube. Aspirated fluid was immediately mixed at a 1:1 ratio with 5% sodium bicarbonate and chilled on ice until delivered to the microbiology laboratory. Standard clinical procedures for processing gastric aspirate samples for mycobacteria were performed, including decontamination with MycoPrep (BBL). The concentrated specimen was plated onto culture medium (Lowenstein-Jensen slants and MB-BacT system [Organon Teknika]) and onto slides. Cultures were incubated at 35 to 37°C for 42 days; slants were monitored weekly while liquid cultures were continuously monitored for growth. Growth in either slant or liquid medium was reported as positive. Slides were stained with a fluorochrome stain (auramine rhodamine) and a Ziehl-Neelsen stain and examined for acid-fast bacilli.

ESR. Disposable Wintrobe tubes, 115 by 3 mm (inside diameter) (Chase Scientific R828B), were used to measure ESR on serial whole blood samples. Whole blood anticoagulated in EDTA was pipetted into the tubes to the 0 graduation line, and the tubes were incubated in the rack for 1 h at room temperature. The distance in millimeters that the red cells sedimented down through the plasma in 1 h was recorded as the ESR. All samples were tested in duplicate.

LPAs. Peripheral blood mononuclear cells (PBMC) were purified from serial blood samples over Percoll gradients, washed, and resuspended in Aim-V medium (Invitrogen). Cells were aliquoted to wells of 96-well U-bottomed plates (Costar) at 2×10^5 cells/well in a final volume of 200 μ l/well. Cells were

stimulated with phytohemagglutinin (PHA; 5 μ g/ml; Sigma, St. Louis, Mo.), PPD (10 μ g/ml; Veterinary Laboratories Agency, Addlestone, Surrey, United Kingdom), mammalian old tuberculin (Synbiotics), or *M. avium* PPD (10 μ g/ml; Veterinary Laboratories Agency) or were unstimulated. Each stimulation was performed in triplicate wells. Cells were incubated at 37°C with 5% CO₂ for 60 h, and then [³H]thymidine (1 μ Ci/well; Amersham) was added for the final 12 to 18 h of incubation. Cells were harvested onto filters by using a cell harvester, filters were dried, and cells were counted in a scintillation counter. Results are reported as stimulation index (SI), the fold increase in counts per minute over the unstimulated control.

Necropsy procedures. Prior to necropsy, animals were anesthetized with ketamine or tiletamine-zolazepam, bled maximally from the femoral vein with the Vacutainer system described previously, and humanely euthanized with an intravenous overdose of sodium pentobarbital. The thoracic cavity was entered sterilely without severing the diaphragm, and the gross extent of mycobacterial infection was recorded. The trachea and attached heart-lung block were then removed from the thoracic cavity and placed in a sterile tray for dissection and evaluation. Each lung lobe was dissected, and the gross dissemination of mycobacterial infection (e.g., number of grossly visible granulomas) as well as other pathological findings was recorded. All mediastinal and tracheobronchial lymph nodes were collected and evaluated for infection. Lung lobes, as well as other tissues, were sectioned and also homogenized to obtain cells and determine bacterial numbers. Grossly visible granulomas were dissected from tissues, particularly lung lobes, and homogenized to obtain cells and to determine bacterial numbers. The brain was removed and sectioned; serial sections were examined for central nervous system involvement and evidence of meningitis. Selected pieces of pulmonary, lymphatic, and other organ tissue were preserved in 10% formalin for histopathological examination.

Histological analysis. Tissue samples at necropsy were fixed in 10% formalin, routinely processed, and embedded in paraffin. Standard sections at 6 μ m were cut and stained with hematoxylin and eosin (H&E), Ziehl-Neelsen stain (for acid-fast bacilli), and von Kossa stain for calcium. Sections from each monkey were analyzed by a board-certified pathologist (E.K.).

Bacterial number determination at necropsy. Tissue was obtained from various sites, including each lung lobe, lymph nodes, spleen, and liver. Visible granulomas within the tissues were also dissected. Tissue pieces were placed into sterile RPMI medium in preweighed tubes, and the weight of tissue was recorded. Tissue was ground in a MediMixer (BD Bioscience, San Jose, Calif.) with the addition of ~3 ml of sterile phosphate-buffered saline. Tenfold dilutions of this homogenate were plated on 7H10 agar plates (Difco) and incubated at 37°C with 5% CO₂, and CFU were counted after 4 weeks. BAL fluid was also diluted and plated on 7H10 agar to determine total numbers of CFU.

RESULTS

Infection of cynomolgus macaques with *M. tuberculosis*. The initial goal of this study was to develop a nonhuman primate model of *M. tuberculosis* infection that reflected this infection and the course of disease in humans. To this end, a low dose of virulent *M. tuberculosis* was delivered directly to the lungs of monkeys via bronchoscope. A total of 17 cynomolgus macaques were infected with ~25 CFU of *M. tuberculosis* strain Erdman, in three separate experiments. All monkeys had evidence of infection in at least one assay, as described below. Based on the clinical data obtained during the course of infection and at necropsy for those monkeys that had been euthanized, the monkeys were grouped into the following categories: 1, rapid progressor to fulminant disease; 2, active-chronic infection; and 3, no disease-latent infection (Table 1). To date, 4 of the 17 animals inoculated were humanely euthanized due to advanced pulmonary mycobacterial infection, 1 was euthanized due to ocular tuberculosis, 4 animals were euthanized at predetermined time points, and 8 of the animals are still alive and in good health at 15 to 21 months postinfection (Table 1). The animals euthanized for advanced pulmonary disease exhibited anorexia and weight loss (13 to 27% from baseline weight). One monkey had tachypnea, and three had a persis-

tent cough. For the monkeys euthanized at predetermined time points, one monkey had lost weight (10% from baseline), but three had gained weight postinfection. Of the remaining living monkeys, one has lost weight, while the remainder have maintained their weight or have gained weight. Regardless of disease state, no apparent extrapulmonary organ dysfunction was noted, and no significant changes in renal values, liver values, or electrolyte levels were observed.

Peripheral blood diagnostic tests. As an indirect measure of inflammation, ESRs were determined for each animal on a biweekly basis for 2 months, then monthly. Prior to infection, the ESR was <2 mm for all the monkeys. Five of 17 monkeys had an elevated ESR within 6 weeks of infection (data not shown). For the rapidly progressing monkey (153-00), the ESR was elevated at 31 days and remained elevated until the time of necropsy. The other four animals with initially elevated ESRs returned to baseline by 8 weeks postinfection (data not shown). Monkeys with other indications of disease progression also had increased ESR. For example, monkey 72-00 began to have an elevated ESR approximately 6 months postinfection, and it was much higher by 10 months postinfection, when he began to show increased signs of disease.

The results of traditional diagnostic tests (i.e., complete blood count with differential and chemistry panels) proved to be relatively nonspecific and of no use in predicting the disease progression of an infected monkey. Several animals exhibited a transient neutrophilia during the acute phase of infection consistent with a common initial response to a bacterial infection. Once this neutrophilia resolved, no other abnormalities were noted on the differentials. The only response noted on chemistry panels was peritremal or terminal hypoproteinemia. This response was noted in the animals that had lost substantial body weight and was most probably the result of prolonged anorexia.

Tuberculin skin testing. Tuberculin skin testing was performed on a biweekly basis for the first 2 to 3 months, then monthly. Both palpebral and abdominal skin testing with mammalian tuberculin were performed. Thirteen of the 17 animals became palpebral skin test positive (grade 4+ or 5+) by 4 to 6 weeks postinfection, and two animals became palpebral skin test positive by 12.5 weeks postinfection (see Table 3). The remaining two animals never exhibited a palpebral skin test result greater than grade 3+. None of the animals in this study had a palpebral skin test result of >1+ prior to infection. In an informal survey of ~200 noninfected macaques tested quarterly over a 2-year period in the Primate Facility for Infectious Disease Research at the University of Pittsburgh, tuberculin skin test results with a grade of >2+ were extremely rare (data not shown). Therefore, a palpebral test reading of grade 3+ was interpreted as positive in our study. Palpebral skin test reactions in the *M. tuberculosis*-infected monkeys were variable after first positivity, often regressing to negative at one test and returning to positive at the next testing period (Fig. 1).

Abdominal skin test results, if positive at all, peaked at 4 to 8 weeks postinfection and then waned (Fig. 1 and data not shown). A positive palpebral test did not necessarily correlate with an abdominal reaction, and vice versa. Nine of the animals were skin tested on the abdomen with standard human-use PPD 4, 6, and 8 weeks postinfection. None of the animals

tested with PPD exhibited any reaction at any time point; therefore, abdominal skin testing with PPD was terminated.

LPA. As an additional assay for an immune response to infection, LPAs with PBMC were performed biweekly for the first 3 months and every 1 to 3 months thereafter. PPD was used to stimulate the cells, as well as *M. avium* PPD and mammalian tuberculin. Monkeys had uniformly low responses to both PPD and *M. avium* PPD prior to infection. After inoculation, PBMC from monkeys responded to both PPD preparations, as well as mammalian tuberculin (Table 2 and data not shown). This was likely due to the overlap in antigens between these two mycobacterial species or the possibility that monkeys had been previously exposed to *M. avium* in the environment and that this response was boosted upon infection with *M. tuberculosis*. Results from PPD-stimulated cells were more consistent than those from mammalian tuberculin-stimulated cells, probably because of the cruder preparation of mammalian tuberculin than of human-use PPD; for this reason, only responses to PPD are shown in Table 2.

Monkeys varied to a large extent with respect to SI, but this did not correlate with disease state or outcome (Tables 1 and 2). All monkeys responded with an SI of >5 by 8 weeks postinfection (Table 2). Fourteen of 17 monkeys showed positive responses as early as 2 weeks postinfection. The LPA response was positive earlier than the tuberculin skin test for all monkeys (Table 3). The peak response was within 8 to 12 weeks postinfection for 16 of 17 monkeys. Most monkeys had a waning of the initial response, and the responses were inconsistent for each monkey. Negative responses were observed after previously positive responses, and these did not appear to correspond to disease status. Nonetheless, the LPA results indicated that all monkeys mounted a response to the infection, thus confirming the initial infection.

Radiographic findings. Chest radiographs were performed on a biweekly basis for 8 to 12 weeks postinfection and then every 1 to 2 months thereafter (Table 4). Eleven of the 17 inoculated monkeys initially exhibited pneumonia in the right lung in the first 2 to 8 weeks postinfection, characterized as small focal areas of pneumonia with nodularity (Fig. 2A). Six monkeys did not resolve the initial pneumonia (Fig. 2B; Table 4). Four of these 11 monkeys had negative radiographs by 3 months postinfection and remained negative for at least 6 months. Collapse of the right middle lobe, as well as miliary disease, was observed on radiographs for two animals and confirmed at necropsy. One monkey (152-00) had substantial right caudal and middle lobe pneumonia that persisted for 6 months and then began to clear (Fig. 2A to C). By 9 months postinfection, this animal had negative chest films, which remained negative up to the time of euthanasia (16 months postinfection). However, this monkey presented with a granulomatous process in the right eye at 10 months postinfection, which persisted until necropsy (see below). Monkey 112-01 had negative chest radiographs at 2 months postinfection, until 8 months postinfection, when a cavity was observed in the right cranial and caudal lobes, which spread to the left lobes 2 weeks later (data not shown). The six monkeys without initial discernible pulmonary infiltrates on radiograph had negative chest films throughout the study (up to 20 months in some cases).

Culture for *M. tuberculosis*. Attempts to culture mycobacteria from the infected monkeys were performed on gastric as-

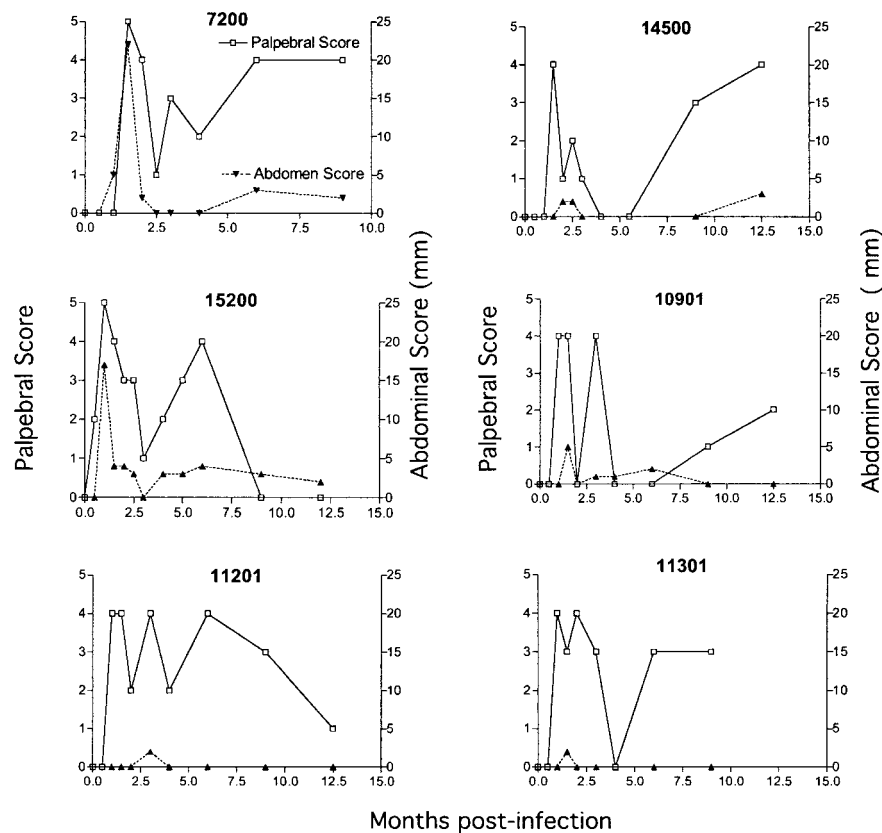


FIG. 1. Tuberculin skin testing results convert to positive shortly after infection with *M. tuberculosis* but are variable throughout the course of infection. Monkeys were injected with 0.1 ml of mammalian tuberculin in the right or left palpebral site or on the abdomen, and the test result was graded from 0 to 5 (for eyelid) or induration was measured on the abdomen in millimeters at 48 and 72 h. Reported here are the 72-h readings for six representative monkeys tested at various time intervals postinfection. Monkey numbers are shown beside symbols on the graph.

pirates and BAL fluid on a regular basis. Nine of 17 monkeys had at least one positive gastric aspirate culture. The five monkeys euthanized due to advanced pulmonary disease had gastric aspirate samples smear positive for *M. tuberculosis* at

necropsy, suggesting that fulminant infection can be detected by this method. However, occasional gastric aspirate samples were positive even for monkeys lacking clinical signs of tuberculosis. At necropsy, gastric aspirate samples from five of seven

TABLE 2. LPAs with PBMC, stimulated with PPD^a

Monkey	0 wk ^b	2 wk	4 wk	6 wk	8 wk	10 wk	3 mo	4 mo	6 mo	9 mo	12 mo
71-00	5	35	9	30	51	204					
72-00	4	— ^c	10	88	25	94	70	34	2	70	
144-00	1	10	2	5	6	6	4	5	5	ND ^d	1
145-00	1	4	3	15	9	7	3	5	2	ND	3
146-00	3	5	2	7	1	9	5	1			
150-00	5	64	15	20	5	18	10	5			
151-00	2	2	1	41	1	10	5	20			
152-00	5	16	92	96	— ^c	— ^c	114	101	19	50	6
153-00	4	7	— ^c	77	— ^c	5					
109-01	0	42	78	66	52	ND	31	38	11	3	
110-01	0	63	51	16	74	ND	13	7	7	2	
111-01	0	36	19	1	38	ND	7	23	9	8	
112-01	3	11	10	13	7	ND	7	15	7	9	
113-01	3	5	2	26	2	ND	25	6	11	13	
114-01	4	46	7	2	3	ND	14	70	22	4	
115-01	2	8	21	1	1	ND	25	15	6	1	
116-01	2	29	54	— ^c	13	ND	70	45	35	7	

^a Data are reported as SIs (fold stimulation over that of cells incubated in medium alone).
^b Preinfection.
^c —, no data reported when PHA (positive-control stimulation with mitogen) did not give a strong SI.
^d ND, not done.

TABLE 3. Comparison of LPA on PBMC with palpebral tuberculin skin test for representative monkeys^a

Monkey	Status	0 wk ^b	2 wk	4 wk	6 wk	8 wk	10 wk	3 mo	6 mo	9 mo	12 mo
72-00	Active-chronic	4 (0)	— ^c (0)	10 (0)	88 (4)	25 (4)	94 (1)	70 (3)	2 (4)	70 (4)	
151-00	Active-chronic	2 (0)	2 (0)	1 (3)	41 (5)	1 (2)	10 (3)	5 (0)			
113-01	Active-chronic	3 (0)	5 (0)	2 (4)	26 (3)	2 (4)	ND ^d	25 (3)	11 (3)	13 (ND)	
152-00	Active-resolved	5 (0)	16 (2)	92 (5)	96 (4)	ND	ND	114	19 (4)	10	5 (0)
146-00	Latent	3 (0)	5 (0)	2 (2)	7 (3)	1 (0)	9 (2)	5 (1)			
109-01	Latent	0 (0)	42 (0)	78 (4)	66	52 (1)	ND	31 (4)	11 (4)	3 (1)	(2)
112-01	Latent-reactivated	3 (0)	11 (0)	10 (4)	13 (4)	7 (2)	ND	7 (4)	7 (0)	9 (4)	
145-00	Latent	1 (0)	4 (0)	3 (0)	15 (4)	9 (1)	7 (2)	3 (1)	5	2 (0)	3
153-00	Rapid progressor	4 (0)	7 (0)	— ^c (5)	77 (2)	— ^c (4)	5	7			

^a LPA data are reported as SIs of PPD compared to medium control. Values in parentheses are the palpebral tuberculin skin test scores, on the standard scale of 0 to 5 (5 being the most strongly positive).

^b Preinfection.

^c —, no data reported when PHA (positive-control stimulation with mitogen) did not give a strong SI.

^d ND, not done.

animals were culture positive for *M. tuberculosis*, and this correlated with the presence of extrapulmonary lesions (spleen or liver). Difficulty in obtaining large quantities of gastric aspirate fluid on a regular basis, particularly from smaller animals, may have contributed to inconsistencies in detecting *M. tuberculosis* in the samples. In the latter months of the study, 5 ml of saline was instilled into the stomach prior to aspirating fluid, which improved the recovery of fluid from the monkeys.

In the first 8 weeks postinfection, *M. tuberculosis* was cultured from the BAL fluid of 10 of 17 monkeys. One additional monkey had a positive BAL culture at 201 days postinfection without advanced disease. After 8 weeks postinfection, BAL cultures were rarely positive unless a monkey was demonstrating signs of advanced disease. Recovery of *M. tuberculosis* from the BAL fluid was inconsistent, as samples from previously positive monkeys were not necessarily positive at subsequent time points. The five monkeys that had consistently negative BAL cultures also did not show signs of progressive tuberculosis (up to 20 months postinfection) and appear to fit in the category of monkeys with clinically latent infection. However, one monkey infected for 20 months with no signs of disease (and categorized as latent) did have a small number of colonies in the BAL fluid at 1 month postinfection but was negative after that. At necropsy, the BAL fluid was positive for *M. tuberculosis* from those monkeys with advanced disease (72-00, 150-00, 153-00, 113-01, and 112-01) and negative from those euthanized without advanced disease.

Cells in the BAL fluid were analyzed by flow cytometry and by manual differential analysis. There was little change in the composition of the BAL fluid over the course of infection in the majority of the monkeys, in terms of percentages of lymphocytes, macrophages/monocytes, and neutrophils. Occasionally, an early increase in lymphocyte percentage was observed. In animals with severe disease, the BAL fluid at necropsy generally had two- to fivefold more cells than BAL fluid samples earlier in infection (data not shown).

Grouping of monkeys with respect to disease progression. Of the 17 monkeys infected to date, different disease progression patterns were observed (Table 1). Here, the three basic categories of disease progression, based on clinical signs, microbiologic cultures, radiographs, and necropsy findings are detailed for representative monkeys in each category.

Rapid progression to disease. As early as 2 weeks postinfection, monkey 153-00 had signs of bronchopneumonia in the

right and left caudal lobes, which progressed to confluent airspace consolidation in the middle and caudal lobes. This monkey had extensive bilateral pulmonary involvement (Fig. 2D). ESR values were elevated by 4 weeks postinfection and reached the highest level (59 mm at 8 weeks postinfection) of any of the infected monkeys. At 4 weeks postinfection, monkey 153-00 began to exhibit moderate anorexia that was subsequently accompanied by progressive weight loss. BAL and gastric aspirate cultures were positive by 6 weeks postinfection. By 8.5 weeks postinfection, the monkey was cachectic and exhibited tachypnea and dyspnea upon ketamine anesthesia. The animal was euthanized at 73 days postinfection due to a persistent deterioration of its clinical presentation. Necropsy of this animal revealed that it had lost 13% of body weight and had disseminated miliary, sometimes confluent, 0.5- to 3-mm granulomas throughout all six lung lobes. Caseation of granulomas in each lobe was noted. Severe hilar and anterior mediastinal lymphadenopathy with caseation necrosis was also evident. Extrapulmonary spread of the disease was noted in the hepatic, splenic, and mesenteric tissue but not in the kidney. Histopathology of the tissues revealed a pattern of lesions consistent with primary pulmonary disease. The presence of

TABLE 4. Thoracic radiograph readings for each monkey^a

Monkey	0.5–2 mo	3–4 mo	6–8 mo	8–10 mo	10–12 mo	12–16 mo
71-00	+/-	+				
72-00	+	—	+	+++		
144-00	+	—	—	—	—	—
145-00	—	—	—	—	—	+/-
146-00	—	—				
150-00	+	++				
151-00	+	+				
152-00	++	++	+	+	—	—
153-00	+	+++				
109-01	—	—	—	—	—	—
110-01	+	—	—	—	—	—
111-01	—	—	—	—	—	—
112-01	+/-	—	—	+++		
113-01	+	++	+++			
114-01	—	—	—	—	+	+/-
115-01	—	—	—	—	—	—
116-01	+	—	—	—	+/-	—

^a Results are indicated as follows: —, negative film; +/-, possibly small area of pneumonia; +, positive; ++ and +++, more extensive involvement. Blank spaces indicate time points postnecropsy.

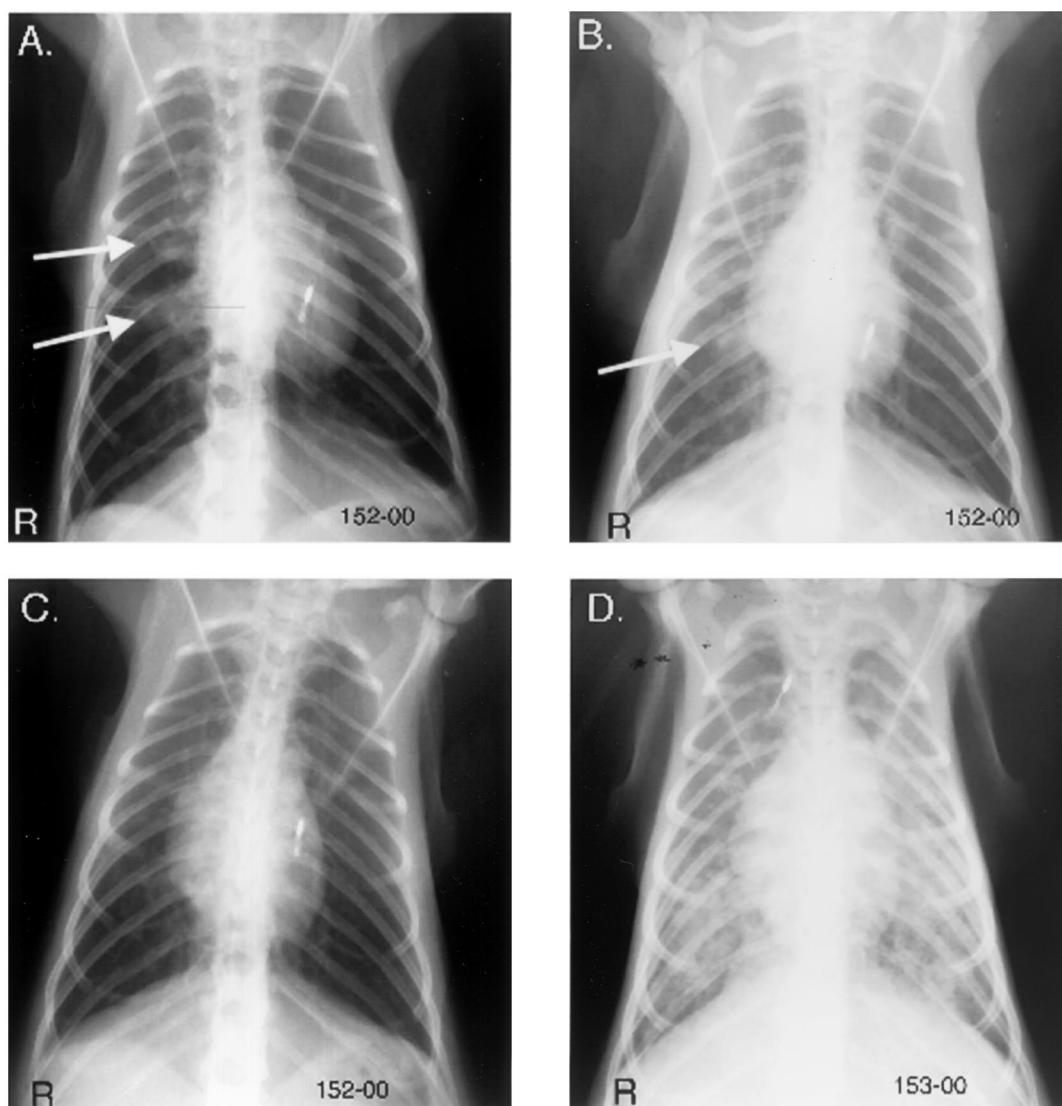


FIG. 2. Chest radiographs from monkeys infected with *M. tuberculosis*. The right side of the monkey is marked on radiographs as "R." (A to C) Monkey 152-00. (A) Four weeks postinfection; note the presence of infiltrate in right lobes (arrows). (B) Seven months postinfection; evidence of disease in right lobes still apparent (arrow). (C) Eleven months postinfection; negative radiograph indicating resolution of disease. (D) Monkey 153-00, rapidly progressing disease, involvement of both left and right sides of lung at 10 weeks postinfection (time of necropsy).

miliary, similarly sized inflammatory foci suggested a lymphohematogenous mode of dissemination. The granulomas had extensive central caseation and were surrounded by epithelioid macrophages (Fig. 3A). Neutrophilic involvement, degree of lymphocytic infiltration, and frequency of multinucleated giant cells were variable. There was often evidence of the necrotizing and inflammatory processes invading by direct extension into larger bronchial airways, and endobronchial spread within lobes was likely to have occurred. Secondary changes in adjacent compressed alveolar airways included extensive edema and marked alveolar histiocytosis. This monkey was classified as a rapidly progressing animal, based on the progression of clinical signs of tuberculosis beginning shortly after infection.

Active-chronic infection. We defined active-chronic infection as persistent evidence of disease, with ongoing radiographic involvement, persistent culture positivity, or other clin-

ical signs of active disease. This category encompassed a wide spectrum of disease and included ~60% (8 of 17) of the infected monkeys. Three examples of monkeys classified as active-chronic infection are presented here. Monkey 151-00 was euthanized at a predetermined time point (4 months postinfection) to observe pathology associated with active-chronic infection prior to end-stage disease. Monkey 113-01 had apparently mild but active infection but later succumbed to advanced tuberculosis. Finally, monkey 152-00 had active-chronic infection and then appeared to resolve the lung involvement by 10 months. These monkeys are detailed below.

Monkey 151-00 was thin with only a fair appetite when inoculated with *M. tuberculosis* but remained weight stable during the course of infection. Radiographically, there was minimal infiltration at the base of the right caudal lobe, with airspace opacification and nodularity, beginning at 4 weeks

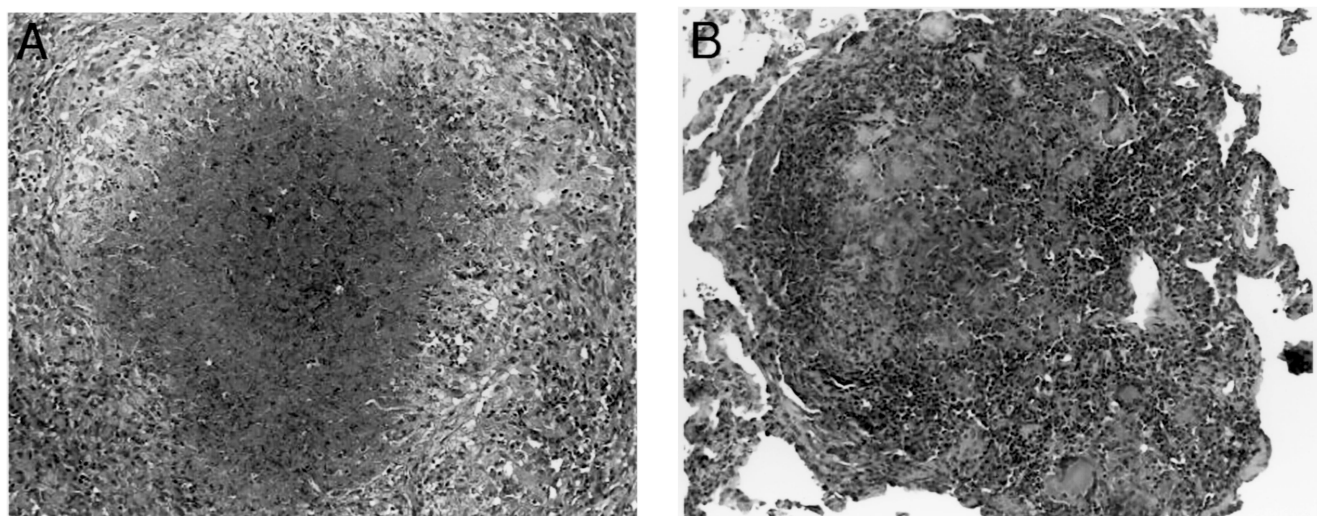


FIG. 3. Lung granulomas from monkeys with active-chronic disease. (A) Granuloma with central caseation from monkey with rapid, progressive disease (153-00). The caseation is surrounded by epithelioid macrophages, and the presence of neutrophils and peripheral lymphocytes is noted. (B) Granuloma from monkey with active-chronic disease, necropsied before progression to advanced disease (151-00). This is an example of a solid granuloma, without central caseation, and shows the presence of multinucleated giant cells, as well as substantial lymphocytic infiltration. Magnifications, $\times 190$. All tissues were stained with H&E.

postinfection but not changing substantially over the course of infection. ESR was elevated at 6 weeks postinfection (15.5 mm) but decreased to baseline levels by 10 weeks postinfection. Gastric aspirate cultures were positive at 6 weeks postinfection, as well as at necropsy. BAL fluid had a low number of CFU (<100) at 2 and 4 weeks postinfection and then was negative. Monkey 151-00 was scheduled for euthanasia at 16.5 weeks postinfection, to observe pathology and disease involvement prior to end-stage disease. At the time of necropsy, the animal was not experiencing any obvious changes in disease status but had definite signs of infection as described above. At necropsy, there were no discernible lesions on the right middle, accessory, and left cranial lobes. The right cranial lobe had a 1.5-cm hemorrhagic lesion on the pleural surface. A modest number of smaller lesions (1 to 2 mm) were observed on the cut surfaces of this lobe, as well as the right caudal lobe. The left caudal lobe had only one visible (~ 2 -mm) granuloma. The right hilar lymph nodes were moderately enlarged. There were >10 granulomas (1 to 4 mm) on the capsule of spleen and on the liver, but the kidneys were unaffected. The pulmonary granulomas in this monkey generally demonstrated a somewhat different histologic pattern than those in monkeys with more advanced disease. Although there were numerous lesions, there were substantially more solid granulomas and less central caseation (Fig. 3B). There was radial palisading of epithelioid cells around granuloma peripheries, and "antigenic points" (a morphological manifestation of antigenic stimulation and hypersensitivity response, observed as long tapering extensions on Langhans cells that are residues of recently fused epithelioid cells) were noted on some of the Langhans giant cells. There was much less caseation overall, compared to monkeys with more advanced disease.

Monkey 113-01 was a large animal and experienced a 5% weight gain over the first 6 months of infection, with no clinical signs of disease. At ~ 30 weeks postinfection, this animal began to lose weight, was mildly anorexic at 33 weeks, and was ca-

chectic at necropsy (34 weeks postinfection), with a 21% weight loss from baseline (preinfection) weight. Persistent coughing developed at 31 weeks postinfection. Radiographic involvement was noted at 2 to 4 weeks postinfection, with acinar shadows spreading along bronchi in the right caudal lobe. By 8 weeks postinfection, there was a poorly defined nodule in the right cranial lobe, and diffuse airspace pneumonia appeared by 16 weeks postinfection. This progressed to airspace consolidation in the right cranial and middle lobes, with the beginning of involvement of the left lobes by 24 weeks. ESR for this monkey was not elevated until the necropsy date (18 mm). The first gastric aspirate positive culture was at 17 weeks postinfection, and the subsequent cultures were inconsistently positive. BAL fluid was culture positive at week 28 and at necropsy. At necropsy, substantial pathological change was noted for all lung lobes. The right cranial and caudal lobes had multiple coalescing caseous granulomas up to 1.5 cm in diameter, and the cranial lobe was extensively adherent to the pleural wall. The left cranial lobe had focal areas of consolidation, with cavitation and caseation evident on cut surfaces. Lymphadenopathy was observed in the hilar and mediastinal nodes, more markedly in the right nodes, and the right hilar node was caseous. A modest number of visible lesions (<10) were observed on liver, spleen, and kidneys. In addition, a caseous lesion extended from the visceral pleura to the parietal surface of an adjacent thoracic vertebra, but histological evaluation revealed that the lesion did not extend into the underlying periosteum. Histologically, the lung sections from this monkey were similar to those described for monkey 153-00 and other monkeys with advanced disease. In general, the lymphocytic infiltrates at the periphery of the granulomas were less pronounced than in monkeys with milder disease.

Monkey 152-00 was also classified into the active-chronic group. This animal remained weight stable throughout the duration of its infection, despite a consistently fair to poor appetite. Right middle and right caudal lobe infiltrate was

detectable on thoracic radiograph by 4 weeks postinfection (Fig. 2A), which progressed up to 12 weeks postinfection and remained stable for an additional 4 weeks (Fig. 2B). However, by 5 months postinfection, the radiographic involvement appeared to decrease slowly, had resolved by 10 months postinfection (Fig. 2C), and remained clear until necropsy at 15 months postinfection. The ESR for monkey 152-00 was elevated at 4 weeks postinfection (13.5 mm) but returned to baseline by 8 weeks postinfection. The ESR increased again at ~10 months postinfection (13.5 mm) and remained at this level until necropsy. Gastric aspirate cultures were positive at 8 weeks postinfection but negative thereafter. The BAL fluid contained a modest number of bacteria (<100 total) at 7 and 20 weeks postinfection but was negative at all other time points, including necropsy. Although the pulmonary involvement appeared to be resolving, at 10 months postinfection this monkey developed anisocoria of the right pupil with particulate matter present in the anterior chamber. Subcorneal granulomas formed and expanded progressively until they caused marked enlargement and distortion of the globe. This ocular infection necessitated euthanasia at 15 months postinfection. There was no obvious involvement of the left eye. Upon necropsy, there was minimal pathology in the majority of lung lobes, although the presence of fibrous adhesions between the right middle lobe and the left caudal lobe and the thoracic wall, in addition to adhesions between the lobes on each side, suggested previous inflammation. A small number (<5) of 1- to 2-mm granulomas were observed in the right cranial and caudal lobes but not in the other lobes. In the right cranial lobe, a pleural granuloma surrounded by hyperemia was suggestive of a Ghon focus. The nearby caseous right hilar node was thought to be the secondary site of transport from this focus with the pair representing a Ghon complex. The spleen had multiple small <1-mm nodular capsular granulomas, while the liver and kidneys had no visible lesions.

Histologically, the lung granulomas in this monkey were consistent with a resolving infection and clearly different than those in monkeys with active disease, with much less caseation observed. In general, the granulomas contained significantly fewer epithelioid macrophages and multinucleated giant cells. Other changes included calcification (confirmed by von Kossa histochemical staining for calcium) of central caseous material in some lesions (Fig. 4A) and the development of more mature, dense fibrous connective tissue (fibrocalcific change). The histology of the affected right eye showed granulomas with caseous necrosis, as well as giant cells. The interior structures of the eye had been destroyed by extensive necrotizing granulomatous inflammation that was consistent with tuberculous panophthalmitis. In summary, this monkey appears to have had an initially progressive pulmonary infection that demonstrated evidence of containment and resolution after a number of months. However, ocular tuberculosis was observed in this monkey, which was apparently not controlled or resolved over time.

No apparent disease (latent infection). We defined this category (no disease) as no radiographic involvement after 4 weeks of infection and no clinical signs of disease for at least 6 months. Approximately 40% of our monkeys were classified into this category. Many of these monkeys survived without

signs of disease for 15 to 21 months, and therefore this class may represent a model of latent infection.

One monkey (146-00) with no signs of disease after infection was chosen for euthanasia at 17 weeks postinfection to examine the extent of pulmonary pathology. This monkey had negative radiographs at all time points postinfection and experienced a weight gain of 22% over the course of infection. ESR was never elevated, and gastric aspirate and BAL fluid cultures were negative at all time points postinfection. The lungs of this monkey contained very few granulomas: one 1-mm granuloma in both the right cranial and middle lobes, three 1-mm focal granulomas in the right caudal lobe, and two 1-mm granulomas in the accessory lobe were observed. The right hilar lymph node showed moderate enlargement and caseation (Fig. 4B), but the left hilar node was normal. No gross lesions were observed in spleen or liver. Histologically, this monkey had few or no lung lesions in most lobes. In the granuloma analyzed from the lung, there were few giant cells and an area of thick fibrosis surrounding central caseation (Fig. 4C and D). The right hilar lymph node had caseous lesions, although not as extensive as in more involved animals, with calcification and peripheral fibrosis (Fig. 4B). In general, the lesions were similar to those of monkey 152-00, described above, but fewer in number.

In summary, this monkey appeared to be controlling the infection and was maintaining only low numbers of bacteria within the granulomas. Presumably this is the case in humans who are latently infected and may reactivate the infection at a subsequent time. Six monkeys remained from this study with clinical presentations consistent with latent infection, infected for 14 to 20 months (Table 1).

Monkey 112-01 was placed into the category of latent infection, based on the absence of clinical or radiographic findings of disease. At 8 months postinfection, this animal began to lose weight and experienced a 20% weight loss over the next 5 weeks, at which time he was euthanized. A severe, persistent cough developed 2 weeks prior to necropsy. This monkey had a positive gastric aspirate at 8 weeks postinfection but was not positive again until 8 months postinfection. BAL culture was also positive at 8 weeks postinfection but was not positive again until necropsy. Radiographically, a subtle area of opacity in the right caudal lobe was detected at 8 weeks postinfection but cleared by 12 weeks. Radiographs were negative up to almost 9 months postinfection, when evidence of disease was observed as bronchopneumonia in the upper cranial lobe spreading into the right caudal lobe. In addition, a thin-walled cavity was observed in the apex of the right cranial lobe. Ten days later (day of necropsy), the radiograph revealed bilateral pulmonary dissemination, with evidence of an open cavity in the right apex. At necropsy, signs of severe disease were noted. Multiple large and small granulomas were observed in all lobes of the lungs. The right cranial lobe had a large suppurative (~5-cm) cavity. This was not observed in the active-chronic monkeys at necropsy and may represent a reactivated lesion. Confluent granulomas with areas of consolidation were observed on the surface of the right caudal lobe, with multiple 1-mm miliary lesions throughout the lobe. The right hilar lymph node was very large, compressing the bronchus entering the right cranial lobe. The left lobes had fewer granulomas than the right lobes, but 1- to 3-mm granulomas were observed in left cranial and

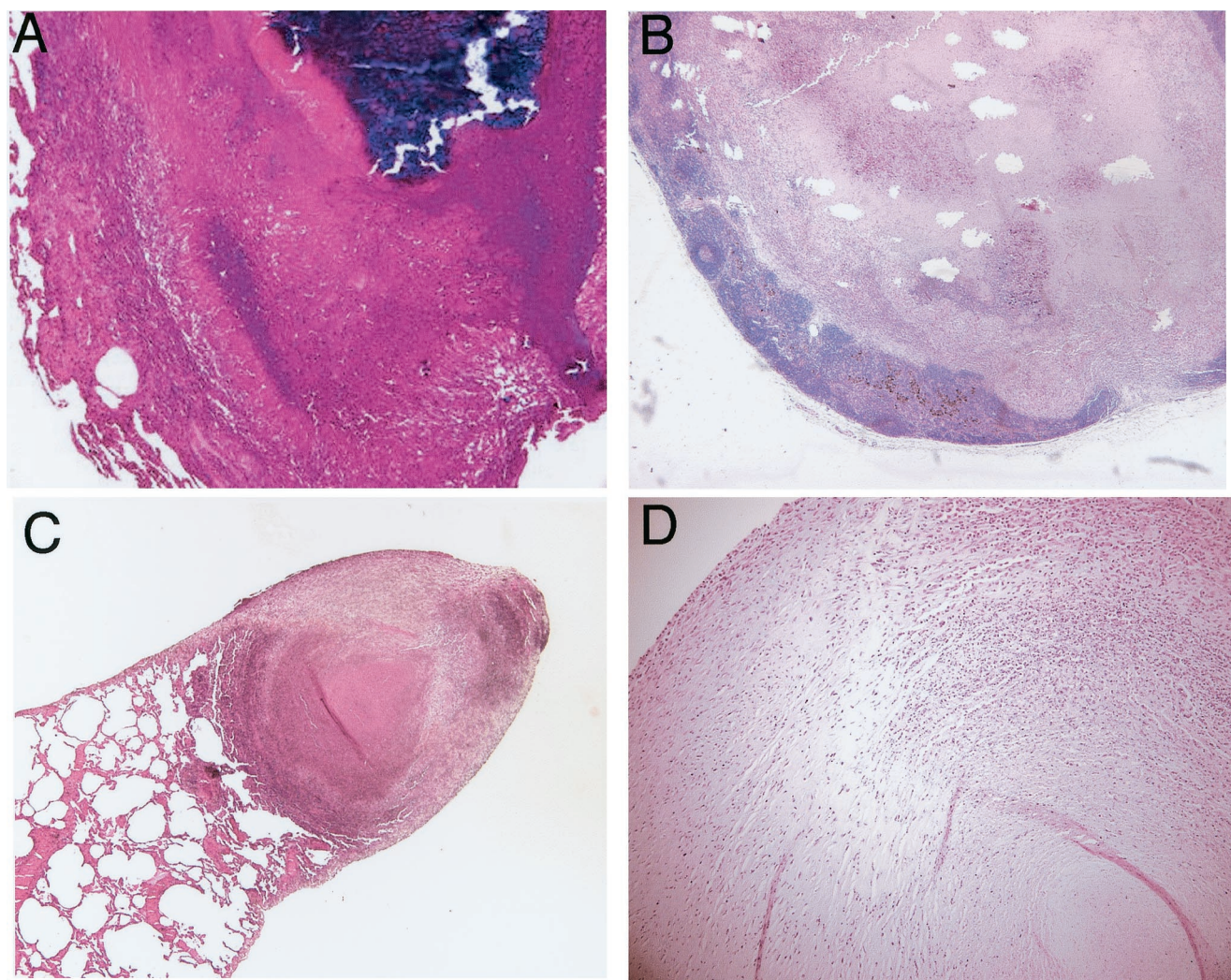


FIG. 4. Granulomas from monkeys with resolving or latent infection. Overall, the granulomas had fewer epithelioid macrophages and giant cells. (A) Mineralization (confirmed as calcification by von Kossa staining [data not shown]) of central caseous material of lung granuloma from a monkey with resolving lung disease (152-00). Magnification, $\times 196$. (B) From monkey 146-00 (apparent latent infection), right hilar lymph node section showing extensive nodal effacement with caseous necrosis and focal areas of early mineralization. Magnification, $\times 98$. (C) Lung granuloma from monkey 146-00, with less caseation than in more advanced monkeys, and development of progressive, dense fibrous connective tissues and reduced lymphocytic infiltration, consistent with containment of infection. Magnification, $\times 19.6$. (D) Higher-power magnification ($\times 196$) of dense, organized fibrotic tissue surrounding granuloma. All tissues were stained with H&E.

caudal lobes. There were no gross lesions on spleen, liver, or kidneys.

Histologically, the right lung lobes showed multifocal and coalescing caseating granulomas. The granulomas had thick bands of lymphocytic cells surrounding central caseation. There was no obvious mineralization in the granulomas. Large cavitory lesions with necrosis were observed, with infiltration into airways. Other sections of the lung had histologic findings consistent with tuberculous pneumonia with epithelioid macrophages, lymphoid infiltrates, and little evidence of caseation or granuloma structure organization.

Extrapulmonary disease. Extrapulmonary spread was variable among monkeys. Monkeys with advanced disease exhibited extrapulmonary dissemination at necropsy. However, active-chronic monkeys that were euthanized prior to advanced disease did not necessarily have visible lesions or *M. tubercu-*

losis in the spleen or liver. In one monkey with active-chronic infection, renal involvement was observed. No skeletal involvement was observed in any of these monkeys, in contrast to previously published data in a similar model (30). As noted above, monkey 152-00 had ocular tuberculosis, which has been reported previously for monkey colonies (31). Each brain was sectioned and examined for evidence of mycobacterial disease, including meningitis. No acid-fast bacilli were found in any of the brain sections examined, and brain histology was normal.

Bacterial load in tissues of monkeys at necropsy. In general, bacterial load in the tissues of these monkeys paralleled disease severity. Monkeys euthanized due to severe, active disease (e.g., monkeys 72-00, 153-00, 112-01, and 113-01) had high bacterial numbers in all lobes of the lung (Table 5). In contrast, the necropsied monkey with latent infection (monkey 146-00), as well as the monkey that appeared to be resolving infection

TABLE 5. *M. tuberculosis* CFU numbers in various monkeys at necropsy^a

Monkey	Category	Granuloma ^b		Right lower or middle lung ^c	Left upper lung ^c	Left hilar lymph node ^c	Right hilar lymph node ^c
		no. 1	no. 2				
72-00	Active-chronic; advanced disease at necropsy	6.2×10^4	2.2×10^6	2×10^4	8.3×10^3	8.4×10^2	1.2×10^4
112-01	Latent, then severe disease	1.9×10^7	2.8×10^5	3.7×10^4	4.4×10^5	ND ^d	4.4×10^6
152-00	Active-chronic then resolving	4.8×10^3	0 (all others)	2.6×10^3	0	0	0
146-00	Latent	1.1×10^3	ND	0	0	0	1.5×10^3

^a Tissue was homogenized in saline, dilutions were plated on 7H10 plates, and plates were read after 21 to 28 days of incubation at 37°C with 5% CO₂. Data for representative monkeys of each category are shown.

^b CFU in entire granuloma; 1 and 2 refer two different granulomas.

^c CFU per gram of tissue.

^d ND, not done.

and moving toward a latent state (monkey 152-00), did not have recoverable bacteria in most lung sections. The few small granulomas recovered from the lungs of monkey 146-00 had ~1,000 CFU, which was 50- to 10,000-fold lower than granulomas from monkeys with advanced disease (Table 5). The right hilar lymph node from monkey 146-00 also contained *M. tuberculosis* (1.5×10^3 CFU). All other samples from monkey 146-00 were negative for *M. tuberculosis*. For monkey 152-00, one granuloma contained bacteria (~5,000 CFU) as did two other specimens from the right lung. All other specimens from this monkey were negative.

DISCUSSION

The nonhuman primate represents an opportunity to study *M. tuberculosis* pathogenesis, disease, and pathology in an immunologically tractable host that is very closely related to humans. Our goal was to develop a nonhuman primate model of tuberculosis that would be useful for a variety of applications. Using a low-dose inoculum, we have recapitulated the various outcomes of human *M. tuberculosis* infection, including primary tuberculosis (active-chronic infection, rapidly progressive in one case), apparently latent infection, and resolving infection. In addition, one of the monkeys appears to have spontaneously reactivated a latent infection. We have extended the studies of others with cynomolgus monkeys as a model (14, 30), by demonstrating that there can be a variety of outcomes of low-dose infection and that some monkeys can control an infection with no apparent signs of disease for >21 months. We also demonstrated that cynomolgus macaques tolerate serial BAL, even with ongoing *M. tuberculosis* infection. With such a model, it is possible to address questions of granuloma formation and pathology and immune responses leading to progressive or latent infection. This model, or variations on it, can be used to test candidate vaccines (including postexposure vaccines), drugs, and diagnostics prior to human clinical trials. In addition, studies of pathogenic mechanisms of *M. tuberculosis*, including expression of virulence factors, gene expression during active or latent disease, and the importance of certain genes in survival or pathogenesis of the organism, can be approached in a model with many similarities to humans.

Similarly to the spectrum of clinical disease progression shared by monkeys and humans, these animals also demon-

strated many comparable gross and microscopic pathological changes consistent with different disease stages in people. Although there was substantial overlap, the histological findings generally reflected the immunological state of dynamic balance between host defenses and progression of disease. Caseation necrosis, a constant factor in active tuberculosis, was more prominent in animals with rapidly progressing infection. Activation of macrophages is essential for a granuloma to destroy microorganisms, and microscopic evidence of this was noted to a greater extent in the more contained state of active-chronic infection. In addition to local immunologic responses, organism containment in healing granulomas is associated with the progressive development of fibrotic and calcific changes—as was seen in monkeys with latent infection. Calcification of lesions from monkeys with long-term, nonprogressive infections was observed histologically (and confirmed by specifically staining sections for calcium), although the calcified lesions were not observed on radiographic films of the monkeys, possibly due to the relatively small size of these lesions.

It has been reported previously that lower doses of *M. tuberculosis* (10 to 100 CFU) can result in cynomolgus macaques with few or no clinical signs of disease, but these studies involved a small number of monkeys and the animals were monitored for only 6 months (30). In addition, it is clear that a larger inoculum (3,000 CFU) causes progressive disease in most, possibly all, cynomolgus macaques (14, 30). A higher dose of organisms than that used in the present study will be necessary for challenge following vaccination. The model we have developed will be most useful for studies of various aspects of the bacterial response as well as the immune response during tuberculosis (active or latent), and the information gathered will be important in determining the mechanisms of protection in vaccine studies.

Low-dose infection with the virulent laboratory Erdman strain of *M. tuberculosis* was achieved via bronchoscope, a relatively noninvasive process. A battery of tests was performed to confirm infection. We assumed infection of a monkey if there was (i) conversion to a positive palpebral or abdominal tuberculin skin test, (ii) increased PBMC lymphocyte proliferation to mycobacterial antigens (PPD), (iii) culture-positive results from gastric aspirate or BAL fluid, or (iv)

pulmonary infiltrate observed on radiograph. All 17 monkeys were judged to be infected by at least one of these criteria.

Tuberculin skin testing is the standard for screening for *M. tuberculosis* or *Mycobacterium bovis* infection in nonhuman primate colonies, as well as in human populations. In nonhuman primate colonies, it is widely recognized that this test can give both false-positive and false-negative results. In our study, all monkeys did convert to a positive tuberculin test (15 of 17 grade 4+ or 5+ and 2 of 17 grade 3+) within a relatively short time postinfection (most by 6 weeks postinfection). Palpebral skin test reactions were variable after first positivity, often regressing to negative at one test and returning to positive at the next testing period. Positivity of tests was not predictive of severity of disease at necropsy, and negative or decreased scores did not necessarily correlate with changes in the lymphocyte proliferation assay performed on peripheral blood cells. The abdominal tuberculin skin test was also variable among monkeys and did not necessarily correlate with the palpebral test administered at the same time. It is evident that clinicians and primate colony managers must reconsider the use of the abdominal tuberculin skin test as a confirmatory test after a positive palpebral test, as it proved to be consistently less positive than the palpebral test and waned markedly in the animals where it was positive during the acute stages of infection. Furthermore, BAL fluid from infected animals was often negative on culture, even though this test is currently considered a good screening test for the presence of *M. tuberculosis* infection (28). However, BAL culture was positive for *M. tuberculosis* in all cases of advanced disease at necropsy. Gastric aspirate cultures were more often positive from infected monkeys and even occasionally in monkeys with no signs of disease. This appears to be a more useful method for detecting *M. tuberculosis* in monkeys suspected of having tuberculosis. ESR, although a nonspecific measure of inflammation, can be an useful indicator of progressing tuberculosis.

Lymphocyte proliferation to PPD was also used to assess peripheral T-cell responses to *M. tuberculosis* infection. In this assay, the majority of monkeys were positive by 2 weeks postinfection, much sooner than the tuberculin skin test. However, a waning of the initial response was observed in a large proportion of animals, and the subsequent responses were inconsistent for each monkey. Negative responses were observed after previously positive responses, and these did not appear to correspond to disease status. Monkeys with active disease did not necessarily have higher or more consistently positive or negative responses than those monkeys with minimal disease. Nonetheless, the LPA results indicated that all monkeys mounted a response to the infection, and this response peaked and then waned or was variable throughout the course of infection. In a number of instances, a negative skin test in a monkey was accompanied by a relatively high SI in the LPA (examples are shown in Table 3). Therefore, it is not possible to conclude that a negative skin test is the result of an "anergic" animal or an animal with an inadequate T-cell response in the periphery. These data agree with published data on the inadequacies of the tuberculin skin test as a diagnostic tool for *M. tuberculosis* infection in nonhuman primates (4, 6, 27, 29) and point to similar problems with LPA as a diagnostic tool.

Approximately 60% of monkeys developed active-chronic infection, with one of these monkeys rapidly progressing to

disease. Active-chronic disease was defined by a number of criteria, including clinical signs of disease (e.g., anorexia and weight loss) and importantly, positive chest radiographs. These monkeys had early infiltrates in the lungs, which did not generally resolve. However, many of the monkeys presented with active infection that was relatively stable for a number of months. Monkey 72-00, for example, had modest disease for up to 9 months before progressing to advanced disease in the remaining month. Monkey 113-01 had mild disease for approximately 6 months and then progressed rapidly to fulminant infection. Thus, the state of active disease can continue in a chronic state indefinitely without apparent distress to the monkey. In contrast to the other monkeys with active infection, monkey 153-00 progressed very rapidly to advanced tuberculosis and was euthanized at 10 weeks postinfection. Bacterial numbers within the dissected granulomas as well as in lung and associated lymph node tissue were fairly high. Dissemination to spleen, liver, and other organs was variable among monkeys and did not necessarily correlate with severity of lung involvement. The differences between rapid and relatively slow progressors may lie in genetics, immunology, prior health status, or other factors. Such a model provides the opportunity to compare monkeys with disease progression differences to determine the factors contributing to different outcomes.

One monkey with active-chronic infection (152-00) showed signs of disease for approximately 9 months and then appeared to recover. Upon necropsy, there were relatively few bacteria in the lungs, and many of the apparent granulomas were not culture positive. The histology from this monkey also was consistent with a healing infection. This monkey apparently represents self-resolving tuberculosis, which can also be observed in humans with tuberculosis. However, this monkey also presented with ocular tuberculosis 9 to 10 months postinfection, which did not resolve with time. Progressive, isolated-organ tuberculosis is described in humans and may occur in any tissue initially affected by earlier dissemination. In this clinical manifestation, lymphatic or hematogenously disseminated organisms are contained or destroyed in other sites but grow progressively in the site in question as an isolated tuberculous process.

Approximately 40% of the monkeys exhibited no signs of disease throughout the study. In some monkeys, an early infiltrate was observed on the thoracic radiographs, but this resolved by 4 to 8 weeks postinfection, and the radiographs remained negative after that time. These monkeys were weight stable or gained weight during the study. Six monkeys remained alive and in good health, with no signs of tuberculosis, 15 to 21 months after initial infection. One monkey was necropsied to determine the extent of infection 4.5 months postinfection. In this monkey, there were only a few small granulomas visible on the lung tissue, both grossly and microscopically. These granulomas contained relatively few bacilli, and no organisms were found in other tissues, except in the right hilar lymph node. The granuloma observed histologically was fibrotic, with a caseous center. Clearly, this monkey was controlling the infection. The actual classification of latent *M. tuberculosis* in monkeys is difficult, since there are no clear indications of the extent of viable bacteria in humans with latent infection. Nonetheless, these monkeys fit the clinical description of humans with latent *M. tuberculosis* infection: conversion of skin

test to tuberculin positive, immunologic evidence of exposure to *M. tuberculosis*, no clinical signs of disease, and the presence of granulomas on necropsy. It remains to be seen whether these monkeys can be experimentally reactivated.

Although we have not attempted experimental reactivation, one of our monkeys judged to be latently infected for 8 months began to show signs of active disease and quickly progressed to advanced tuberculosis. A large cavity was observed in the right cranial lung lobe by radiograph and at necropsy, which would be consistent with reactivation of a latent infection in humans. Radiographically, the infiltrate was observed at 8 months postinfection in the right cranial and middle lobes and rapidly advanced to the right caudal and then left lobes. In addition, the pattern of tiny granulomas over the pleural surface of the lungs at necropsy was consistent with spread from a main lesion, such as the cavity. Although we cannot exclude the possibility that this monkey may have been reinfected from another monkey and rapidly progressed to disease, it also remains a strong possibility that spontaneous reactivation of a previously latent infection resulted in advanced disease.

In summary, we have developed a nonhuman primate model that appears to represent in a relatively small number of monkeys the entire spectrum of human *M. tuberculosis* infection. In particular, a subset of monkeys presented with no clinical signs of disease, a state likely representing latent infection. Since latent tuberculosis is difficult to model in animals, this represents a step forward in the study of latent infection. This model has distinct advantages over other animal models in terms of a close resemblance to human disease, a wide array of immunologic reagents for the study of these monkeys, and pathology very similar to that seen in human tuberculosis. The disadvantages include the expense and difficulty of maintaining monkeys, particularly in a biosafety level 3 facility. Although the outbred nature of macaques can be viewed as a limitation on performing some studies, this also likely contributes to the wide range of clinical manifestations of tuberculosis seen in this model.

ACKNOWLEDGMENTS

This research was supported by National Institutes of Health grants RO1 AI47485 and RO1 HL68526 (J.L.F.) and an Infectious Disease Society of America Harold Neu/Bayer Research Fellowship Award (P.L.L.).

We are grateful to Michael Murphey-Corb and the staff at the University of Pittsburgh Primate Facility for Infectious Disease Research for assistance and support in establishing the biosafety level 3 nonhuman primate facility. We thank Dawn McClemons-McBride for facilitating the ordering and shipping of monkeys. We are indebted to Clayton Wiley and Charleen Chu for assistance in brain and ocular histology, to Chirag Shah for examination of the tuberculous eye, and to the members of the Flynn laboratory for helpful discussions. In particular, we are grateful to Holly Scott for assistance in preparation of figures. We also thank the Division of Laboratory Animal Research at the University of Pittsburgh for care of the animals.

REFERENCES

- Barclay, W. R., W. M. Busey, D. W. Dalgard, R. C. Good, R. W. Janick, J. E. Kasik, E. Ribic, C. E. Ulrich, and E. Wolinsky. 1973. Protection of monkeys against airborne tuberculosis by aerosol vaccination with bacillus Calmette-Guerin. *Am. Rev. Respir. Dis.* **107**:351–358.
- Bean, A. G. D., D. R. Roach, H. Briscoe, M. P. France, H. Korner, J. D. Sedgwick, and W. J. Britton. 1999. Structural deficiencies in granuloma formation in TNF gene-targeted mice underlie the heightened susceptibility to aerosol *Mycobacterium tuberculosis* infection, which is not compensated for by lymphotoxin. *J. Immunol.* **162**:3504–3511.
- Caruso, A. M., N. Serbina, E. Klein, K. Triebold, B. R. Bloom, and J. L. Flynn. 1999. Mice deficient in CD4 T cells have only transiently diminished levels of IFN- γ , yet succumb to tuberculosis. *J. Immunol.* **162**:5407–5416.
- Chaparas, S. D., R. C. Good, and B. W. Janicki. 1975. Tuberculin-induced lymphocyte transformation and skin reactivity in monkeys vaccinated or not vaccinated with bacille Calmette-Guerin, then challenged with virulent *Mycobacterium tuberculosis*. *Am. Rev. Respir. Dis.* **112**:43–47.
- Cooper, A. M., J. Magram, J. Ferrante, and I. M. Orme. 1997. Interleukin 12 (IL-12) is crucial to the development of protective immunity in mice intravenously infected with *Mycobacterium tuberculosis*. *J. Exp. Med.* **186**:39–45.
- Corcoran, K. D., and G. P. Jaax. 1991. An attempt to predict anergy in tuberculosis suspect cynomolgus monkeys. *Lab. Anim. Sci.* **41**:57–62.
- Dannenberg, A. M. 1994. Rabbit model of tuberculosis, p. 149–156. *In* B. R. Bloom (ed.), *Tuberculosis: pathogenesis, protection, and control*. American Society for Microbiology, Washington, D.C.
- de Jong, R., F. Altare, L.-A. Haagen, D. G. Elferink, T. de Boer, P. van Breda Vriesman, P. J. Kabel, J. Draaisma, J. van Dissel, F. Kroon, J.-L. Casanova, and T. Ottenhoff. 1998. Severe mycobacterial and salmonella infections in interleukin-12 receptor deficient patients. *Science* **280**:1435–1438.
- Flynn, J. L., and J. Chan. 2001. Animal models of tuberculosis. *In* W. N. Rom and S. M. Garay (ed.), *Tuberculosis*, 2nd ed., in press. Lippincott Williams & Wilkins, Philadelphia, Pa.
- Flynn, J. L., and J. Chan. 2001. Immunology of tuberculosis. *Annu. Rev. Immunol.* **19**:93–129.
- Flynn, J. L., M. M. Goldstein, J. Chan, K. J. Triebold, K. Pfeffer, C. J. Lowenstein, R. Schreiber, T. W. Mak, and B. R. Bloom. 1995. Tumor necrosis factor- α is required in the protective immune response against *M. tuberculosis* in mice. *Immunity* **2**:561–572.
- Good, R. C. 1968. Simian tuberculosis: immunologic aspects. *Ann. N. Y. Acad. Sci.* **154**:200–213.
- Keane, J., S. Gershon, R. P. Wise, E. Mirabile-Levens, J. Kasznica, W. D. Schwietzman, J. N. Siegel, and M. M. Braun. 2001. Tuberculosis associated with infliximab, a tumor necrosis factor α -neutralizing agent. *N. Engl. J. Med.* **345**:1098–1104.
- Langermans, J. A. M., P. Andersen, D. van Soolingen, R. A. W. Vervenne, P. A. Frost, T. van der Laan, L. A. H. van Pinsteren, J. van den Hombergh, S. Kroon, I. Peckel, S. Florquin, and A. W. Thomas. 2001. Divergent effect of bacillus Calmette-Guerin (BCG) vaccination on *Mycobacterium tuberculosis* infection in highly related macaque species: implications for primate models in tuberculosis vaccine research. *Proc. Natl. Acad. Sci. USA* **98**:11497–11502.
- McMurray, D. 2001. Disease model: pulmonary tuberculosis. *Trends Mol. Med.* **7**:135–137.
- Mohan, V. P., C. A. Scanga, K. Yu, H. M. Scott, K. E. Tanaka, E. Tsang, M. M. Tsai, J. L. Flynn, and J. Chan. 2001. Effects of tumor necrosis factor α on host immune response in chronic persistent tuberculosis: possible role for limiting pathology. *Infect. Immun.* **69**:1847–1855.
- Muller, I., S. Cobbald, H. Waldmann, and S. H. E. Kaufmann. 1987. Impaired resistance to *Mycobacterium tuberculosis* infection after selective in vivo depletion of L3T4⁺ and Lyt-2⁺ T cells. *Infect. Immun.* **55**:2037–2041.
- Orme, I. M., and F. M. Collins. 1994. Mouse model of tuberculosis, p. 113–134. *In* B. R. Bloom (ed.), *Tuberculosis: pathogenesis, protection, and control*. American Society for Microbiology, Washington, D.C.
- Rhoades, E. R., A. A. Frank, and I. M. Orme. 1997. Progression of chronic pulmonary tuberculosis in mice aerogenically infected with virulent *Mycobacterium tuberculosis*. *Tuber. Lung Dis.* **78**:57–66.
- Richter, C. B., N. D. M. Lehner, and R. V. Hendrickson. 1984. Primates, p. 298–383. *In* J. G. Fox, B. J. Cohen, and F. M. Loew (ed.), *Laboratory animal medicine*. Academic Press, Inc., San Diego, Calif.
- Scanga, C. A., V. P. Mohan, K. Yu, H. Joseph, K. Tanaka, J. Chan, and J. L. Flynn. 2000. Depletion of CD4⁺ T cells causes reactivation of murine persistent tuberculosis despite continued expression of IFN- γ and NOS2. *J. Exp. Med.* **192**:347–358.
- Schmidt, L. H. 1955. Induced pulmonary tuberculosis in the rhesus monkey: its usefulness in evaluating chemotherapeutic agents. *Trans. Conf. Chemother. Tuberc.* **14**:226–231.
- Schmidt, L. H. 1956. Some observations on the utility of simian tuberculosis in defining the therapeutic potentialities of isoniazid. *Annu. Rev. Tuberc. Pulm. Dis.* **74**:138–153.
- Schmidt, L. H. 1966. Studies on the antituberculous activity of ethambutol in monkeys. *Ann. N. Y. Acad. Sci.* **135**:747–758.
- Schroeder, C. R. 1938. Acquired tuberculosis in the primate in laboratories and zoological collections. *Am. J. Public Health* **28**:469–475.
- Shen, Y., D. Zhou, L. Qiu, X. Lai, M. Simon, L. Shen, Z. Kou, Q. Wang, L. Jiang, J. Estep, R. Hunt, M. Clagett, P. K. Sehgal, Y. Li, X. Zeng, C. T. Morita, M. B. Brenner, N. L. Letvin, and Z. W. Chen. 2002. Adaptive immune response of V γ 2V δ 2⁺ T cells during mycobacterial infections. *Science* **295**:2255–2258.
- Snyder, S. B., and J. G. Fox. 1973. Tuberculin testing in rhesus monkeys (*Macaca mulatta*): a comparative study using experimentally sensitized animals. *Lab. Anim. Sci.* **23**:515–521.
- Southers, J. L., and E. W. Ford. 1995. Medical management, p. 257–270. *In*

- B. Bennett, C. Abee, and R. Henrickson (ed.), Nonhuman primates in biomedical research: biology and management. Academic Press, San Diego, Calif.
29. **Stunkard, J. A., F. T. Szatalowicz, and H. C. Sudduth.** 1971. A review and evaluation of tuberculin testing procedures used for macaca species. *Am. J. Vet. Res.* **32**:1873–1878.
30. **Walsh, G. P., E. V. Tan, E. C. de la Cruz, R. M. Abalos, L. G. Villahermosa, L. J. Young, R. V. Cellona, J. B. Nazareno, and M. A. Horwitz.** 1996. The Philippine cynomolgus monkey (*Macaca fascicularis*) provides a new nonhuman primate model of tuberculosis that resembles human disease. *Nat. Med.* **2**:430–436.
31. **West, C. S., S. J. Vainisi, C. M. Vygantas, and F. Z. Beluhan.** 1981. Intraocular granulomas associated with tuberculosis in primates. *J. Am. Vet. Med. Assoc.* **179**:1240–1244.
32. **Wolf, R. H., S. V. Gibson, E. A. Watson, and G. B. Baskin.** 1988. Multidrug chemotherapy of tuberculosis in rhesus monkeys. *Lab. Anim. Sci.* **38**:25–33.
33. **Zumpe, D., M. S. Silberman, and R. P. Michael.** 1980. Unusual outbreak of tuberculosis due to *Mycobacterium bovis* in a closed colony of rhesus monkeys (*Macaca mulatta*). *Lab. Anim. Sci.* **30**:237–240.

Editor: V. J. DiRita